A TECHNIQUE TO PREDICT THE AERODYNAMIC LOSSES OF BATTLE DAMAGED WINGS

Thomas W. Pickhaver, Peter M. Render
Department of Aeronautical and Automotive Engineering, Loughborough University,
Loughborough, LE11 3TU, UK
T.W.Pickhaver@lboro.ac.uk

Abstract

Development of a technique to predict the effects of simulated battle damage on the aerodynamics of a three dimensional wing is described. A methodology for converting two dimensional lift, drag and pitching moment data to three dimensional values is developed. To test this methodology, wind tunnel testing was carried out on a three dimensional half model of the NASA LS(1)-0417MOD aerofoil, with simulated battle damage. The effective aspect ratio of the model was 6. A circular hole with a diameter of 20% of wing chord was used to simulate gunfire-type battle damage. To model different attack directions the axis of the hole was inclined along the chord and span. Three spanwise locations for the damage were tested. Testing was undertaken at a Reynolds Number of 1,000,000. Compared to an undamaged wing, the addition of damage caused an increase in drag, a decrease in lift and a more negative pitching moment. The effects increased with incidence and changed with hole orientation. These effects were reduced as the damage was moved towards the wing tip. Results from the predictive technique were compared with those from half model testing. The predicted lift loss was seen to be in close agreement with wind tunnel results, but the drag increase was under predicted. The biggest errors in the prediction occurred for the pitching moment, although the relatively low aspect ratio is believed to have an adverse effect on the comparison.

Nomenclature

b	Wing span
c	Chord
C_D	Three dimensional drag coefficient
C_d	Two dimensional drag coefficient
C_L	Three dimensional lift coefficient
C_l	Two dimensional lift coefficient
C_M	Three dimensional pitching moment coefficient
C_m	Two dimensional pitching moment coefficient
C_P	Three dimensional pressure coefficient
C_p	Two dimensional pressure coefficient
$C_{p\ hole}$	Pressure coefficient loss across the damage hole
dC_D	Three dimensional drag coefficient increment due to damage
dC_d	Two dimensional drag coefficient increment due to damage
dC_L	Three dimensional lift coefficient increment due to damage
dC_l	Two dimensional lift coefficient increment due to damage
dC_M	Three dimensional pitching moment coefficient increment due to damage

dC_m	Two dimensional pitching moment coefficient increment due to damage
LE	Leading edge
Re	Reynolds Number
s	Percentage of span
TE	Trailing edge

Greek

α	Incidence
ΔA_n	Area of a small square
$\Delta C_{p\,n}$	Pressure coefficient across a small square

Subscripts

$2D$	Two dimensional parameter
$3D$	Three dimensional parameter
$3Dc$	Converted three dimensional parameter
damaged	Parameter from damaged wing
undamaged	Parameter from undamaged wing

1 Introduction

Aircraft survivability in combat is an important aspect of the design process. Survivability assessments typically concentrate on structural and system integrity, although it is known aircraft can survive a significant level of damage and continue to fly. Therefore, a need to determine whether the aircraft can complete its mission or should instead return to a friendly base arises. Previous work by the authors [1] has determined the two dimensional aerodynamic characteristics of different configurations of simulated battle damage for a modern low-speed aerofoil, the NASA LS(1)-0417MOD. This paper will analyse the effects on a three dimensional (finite aspect ratio) wing of the same aerofoil section. In addition a technique for using two dimensional data to predict three dimensional values will be developed.

Studies into simulated battle damage effects began with Irwin's work [2], using a two dimensional model of a NACA 64_1-412 aerofoil. Irwin's work focused on circular holes with diameters between 10% and 40% of aerofoil chord. Studies into effects of battle damage on three

dimensional wings were undertaken by Render et al [3]. In addition, this work developed a basic predictive technique for predicting the effects of a three dimensional wing from two dimensional data. It was found that this method broke down when applied to the LS-series aerofoil. The three dimensional testing undertaken by Render et al used a model of the same chord as the two dimensional testing by Irwin, and as such physically identical hole sizes. It was found that a significant limitation of the prediction was that it could not be accurately applied to wings of varying chord.

2 Experimental Setup

2.1 Wind Tunnel Configuration

Testing on a three dimensional model of the NASA LS(1)-0417MOD aerofoil was carried out. Loughborough University's 1.3 m by 1.9 m wind tunnel was used. This wind tunnel allowed for higher Reynolds Numbers to be tested, compared to the two dimensional testing [1]. The model had a of span 975 mm and 325 mm chord and effective aspect ratio of 6. The maximum speed of the wind tunnel was 45 m/s. This gave a Reynolds Number of up to 1,000,000.

The model was mounted vertically in a half-wing configuration, as shown in Figure 1, with the wind tunnel floor acting as a reflection plane. It was connected to a six component under-floor balance by a single strut. Nominal balance accuracy was better than 0.05% full-scale deflection for all axes. A yaw drive system provided incidence control with an accuracy better than $0.1°$. Boundary layer transition was forced through use of a transition strip at 7.5% chord. Balance measurements were supplemented through use of surface flow visualisation and surface pressure measurements. Surface flow visualisation used a mixture of titanium dioxide, paraffin and linseed oil painted onto the wing. Pressure tappings were connected to an array of four Pressure Systems 16TC/DTC pressure scanners, connected to a computer via a Chell CANdaq data acquisition unit with a nominal

accuracy of ± 0.0696 mmH$_2$O.

2.2 Damage Modelling and Model Construction

Damage was modelled using circular holes. Previous studies by Render et al [3] and Robinson & Leishman [4] have shown star shaped damage and actual battle damage are reasonably replicated by circular holes. It was found that the flow features and general aerodynamic effects were consistent with more realistic damage shapes. During this study three parameters were varied between damage cases:

- Hole diameter, expressed as a percentage of the chord.

- Chordwise obliquity – upper and lower holes displaced along the chord.

- Spanwise skew – upper and lower holes displaced along the span.

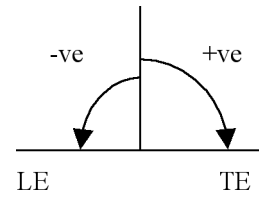Chordwise obliquity involved pivoting the holes about the centre of the aerofoil's chord

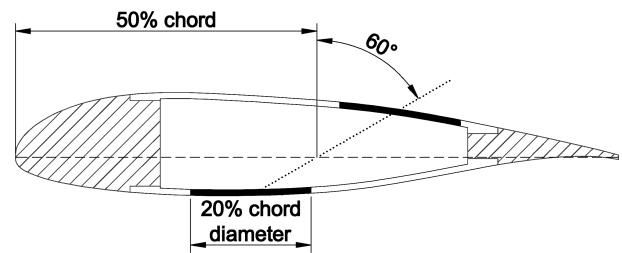**Fig. 2** Sign convention for obliquity angles, taken from vertical

Fig. 3 Chordwise cross-section of the model illustrating the basic cavity configuration and a typical damage hole (+60° obliquity).

line. The sign convention is shown in Figure 2. Positive obliquity was defined as the upper surface hole moving closer to the trailing edge of the model and the lower surface hole moving closer to the leading edge. Figure 3 shows a configuration with positive obliquity. The dashed line indicates the chord line, and the dotted line shows the centre-line of the hole, pivoted about half chord. Positive skew involved the upper surface hole moving closer to the wing tip. All obliquity and skew angles were taken from the vertical.

To remain consistent with the previous two dimensional testing, the wing had a cavity to replicate the internal structure of an aircraft wing. The cavity was between 24% and 75% chord, as shown in Figure 3 (hatched region shows the solid leading and trailing edges), and covered the central 85% of the span. The cavity was included as previous studies [5] had shown its presence had an influence on the aerodynamic effects of battle damage. The cavity was bounded by aluminium spars to increase the strength of the model. The leading and trailing edges were solid and manufactured from ProLab 65, a synthetic modelling board. The upper and lower surfaces of the cavity were bounded by

Parameter	2D Repeatability	3D Repeatability
C_L	± 0.018	± 0.011
C_D	± 0.0016	± 0.0015
C_M	± 0.0021	± 0.0023

Table 1 Summary of experimental repeatability

removable fibreglass panels to which the damage was applied. This allowed for different damage combinations to be tested without manufacturing a new model. All panels were manufactured from the same set of moulds to preserve geometric repeatability and were affixed to the model with countersunk screws. The repeatability of the lift, drag and pitching moment coefficients, as determined from balance measurements, are given in Table 1 for the two dimensional (shown for comparison, to be considered when converting data) and three dimensional models.

To allow the effects of the wing tip vortex on damage to be investigated the removable panels could be installed at three spanwise locations. The "Root" panel location had the panel centre located at 25% span, the "Centre" panel was centred at 50% span and the "Tip" location was centred at 75% span. All panels were interchangeable with each location. A set of three undamaged "datum" panels were used for repeatability checks and were installed in locations where damage was not present to minimise any repeatability errors.

2.3 Summary of Test Cases

The damage cases used during three dimensional testing were:

- 20%c diameter hole, 0° obliquity and 0° skew (from now on referred to as 'straight through').

- 20%c diameter hole, ±60° obliquity and 0° skew.

- 20%c diameter hole, ±45° skew and 0° obliquity.

- Each tested with the holes centred about 25% span, 50% span and 75% span.

2.4 Data Presentation

For ease of presentation, results for damaged cases are presented as coefficient increments. This is defined as the change from undamaged lift, drag or pitching moment coefficients due to the presence of damage. Equations 1 to 3 define the lift, drag and pitching moment coefficient increments respectively. Three dimensional coefficient values are represented by upper case subscripts. Where required, two dimensional coefficient values are represented by a lower case subscript.

$$dC_L = C_{L\ damaged} - C_{L\ undamaged} \qquad (1)$$

$$dC_D = C_{D\ damaged} - C_{D\ undamaged} \qquad (2)$$

$$dC_M = C_{M\ damaged} - C_{M\ undamaged} \qquad (3)$$

2.5 Key Definitions: Weak and Strong Jets

Irwin defined [2] two terms to classify the flow through a damage hole: weak jet and strong jet. Weak jets are typically found with smaller holes at all incidences, or larger holes at lower incidences. Weak jets are associated with smaller coefficient increment values. Strong jets are found with larger holes and higher incidences. Strong jets are typically associated with larger coefficient increments due to the considerably larger wake from the damage hole.

3 Two Dimensional Trends

During two dimensional testing, hole size, obliquity and skew were varied. A detailed discussion of the results and trends from two dimensional testing can be found in [1]. A brief summary of the key trends is provided here. Testing confirmed the general trends identified by Irwin [2], where jet strength increased with incidence. Increasing jet strength was associated with a more negative lift coefficient increment (signifying a greater loss in lift) and a more positive

drag coefficient increment (a greater increase in drag). As the jet strengthened, the pitching moment coefficient became more negative (i.e. nose down).

3.1 Effects of Obliquity

It was found that adding positive obliquity generally weakened the jet and delayed transition to a strong jet to higher incidences. Adding negative obliquity generally increased the jet strength, causing more disruption to the wing aerodynamics. The variation of lift, drag and pitching moment coefficient increments with obliquity are shown in Figures 4 to 6 respectively. The authors' earlier paper [1] provides a detailed analysis of the surface flow visualisation effects for each obliquity case. Lift coefficient increments (Figure 4) became more negative with negative obliquity, and less negative with positive obliquity. Drag coefficient increments (Figure 5) increased as obliquity became more negative. The pitching moment coefficient increments (Figure 6) also became more negative as obliquity became more negative.

It should be noted that the $+60°$ obliquity case exhibited unusual trends. At approximately $+6°$ incidence the jet did not strengthen further, unlike all other oblique cases. The dC_l values became less negative after this point, and the dC_d values remained approximately constant. Surface flow visualisation confirmed that the jet was not developing as with other cases.

3.2 Effects of Skew

Adding skew generally did not have a significant effect on the coefficient increments but surface flow visualisation from [1] showed asymmetry was introduced into the flow. When skew and obliquity were combined the results generally tended towards those of obliquity. The lack of change in coefficient increments due to skew was as a result of the holes remaining in the same chordwise location. Given the two dimensional wing had no spanwise pressure variation there was therefore no change in pressure difference between the upper and lower surfaces at the
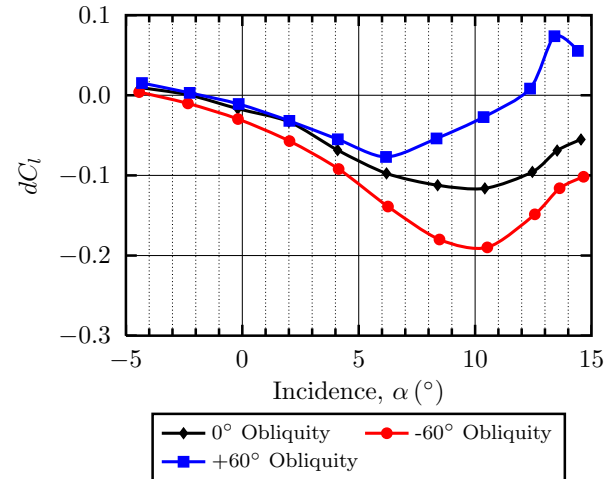

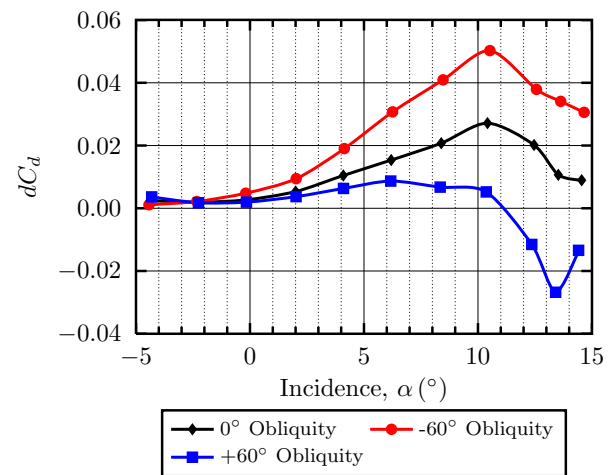**Fig. 4** Variation of two dimensional lift coefficient increments with obliquity

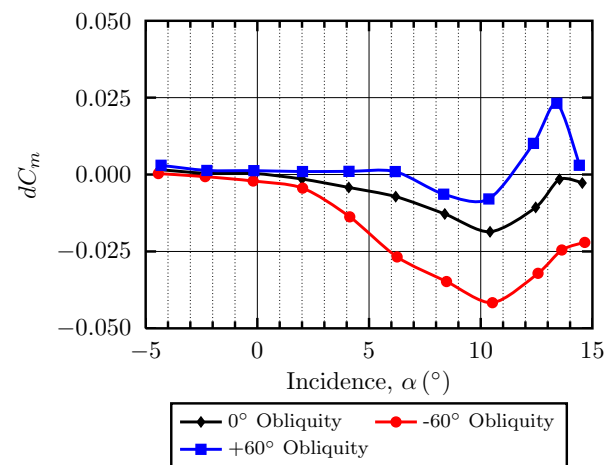**Fig. 5** Variation of two dimensional drag coefficient increments with obliquity

Fig. 6 Variation of two dimensional pitching moment coefficient increments with obliquity

location of the hole with skew.

4 Three Dimensional Trends

Previous work by Render et al [3] had discussed the effects on battle damage of a varying spanwise pressure distribution associated with a three dimensional wing compared to a two dimensional wing, as tested by Irwin [2]. The findings can be summarised as follows:

- Asymmetry was introduced into surface flow visualisation, turning the jet towards the root

- The asymmetry was greatest nearest the tip

- Coefficient increments reduced towards the tip, with the reducing pressure differential

- Transition to strong jet was delayed as the hole was moved towards the tip

4.1 Effects due to Variation of Reynolds Number

With two dimensional testing undertaken at a Reynolds Number of 500,000 and three dimensional testing undertaken at Re = 1,000,000 it was important to assess any potential Reynolds Number effects on the coefficient increments. Therefore, the three dimensional model was tested at both Reynolds Numbers and the 20%c straight through hole used to evaluate any potential effects. Generally the three coefficient increments showed little change with Reynolds Number. This suggests the transition strip was successful in removing any kind of dependency on Reynolds Number.

4.2 Effects of a Finite Span

Figures 7 to 9 show the variation of lift, drag and pitching moment coefficients with span. The lift coefficient increments (Figure 7) show that at the tip location, dC_L had reduced in magnitude significantly. The drag coefficient increments (Figure 8) showed a similar trend. Surface flow visualisation indicated that these effects

were as a result of the jet weakening. This is consistent with findings by Render et al [3]. An unexpected effect was a reduction in dC_L values for the root location, compared to the centre location. Flow visualisation indicated that the boundary layer from the wind tunnel floor was restricting the expansion of the jet. Surface flow visualisation showed the jet being skewed slightly towards the tip, unlike at the tip location, where the jet was being skewed towards the root. This slight reduction of jet strength at the root location is also supported by the dC_D values (Figure 8) which decreased in magnitude, suggesting a smaller wake. An additional effect, when compared to two dimensional data, is that transition points and stalling angles generally occurred at a higher incidence.

4.3 Effects of Obliquity

Due to balance load limitations, testing on the -60° obliquity case was restricted to +11° incidence. Figures 10 to 12 show the lift, drag and pitching moment coefficient increments for a 20%c hole with -60°, 0° and +60° obliquity, at the centre location of the wing. The three coefficient increments follow generally similar trends to the two dimensional studies (Figures 4 to 6). The unique trends identified with the +60° obliquity case are shown as repeatable with the three dimensional model. The dC_L and dC_D values show the jet failing to strengthen (decreasing dC_L, constant dC_D) at a similar incidence, slightly increased to approximately +9°. Despite the different model configurations, the pitching moment coefficient increments (Figure 12) show generally similar trends to the two dimensional data (Figure 6).

4.4 Effects of Skew

Due to the varying spanwise pressure distribution of the finite aspect ratio wing, skew angles either side of the hole centreline were tested. The lift, drag and pitching moment coefficient increments are shown in Figures 13 to 15 for the centre location. Generally, there was little variation in the coefficient increments, as the pressure dif-

Fig. 7 Variation of dC_L with spanwise location for a 20%c straight through hole

Fig. 8 Variation of dC_D with spanwise location for a 20%c straight through hole
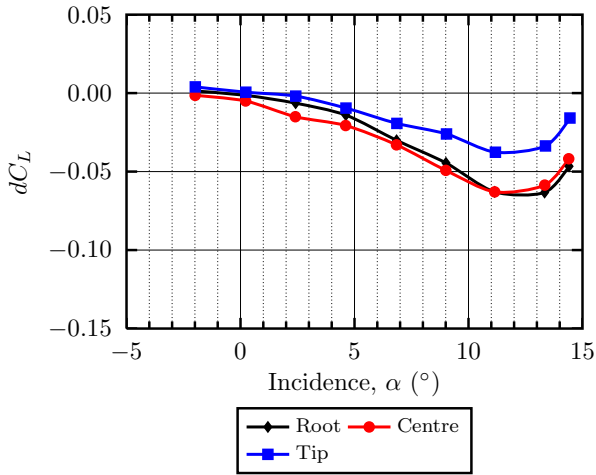

Fig. 9 Variation of dC_M with spanwise location for a 20%c straight through hole

Fig. 10 Variation of dC_L with obliquity for a 20%c hole at the centre location
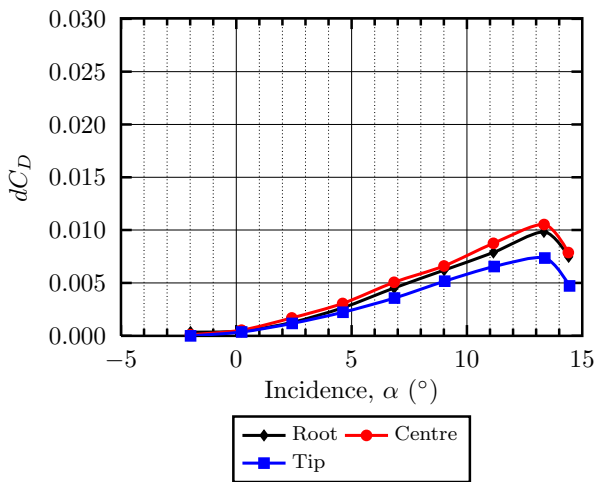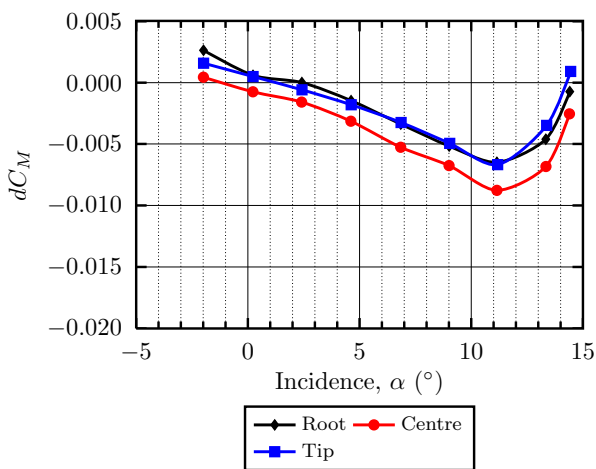

Fig. 11 Variation of dC_D with obliquity for a 20%c hole at the centre location
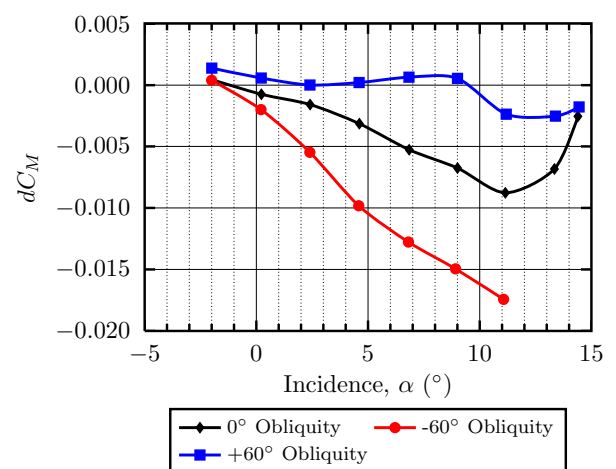
Fig. 12 Variation of dC_M with obliquity for a 20%c hole at the centre location

ference across the holes was relatively constant for the three cases. Some deviation was noted towards stall, due to the increased repeatability bounds. Although there was more variation in the lift coefficient increment, the jet strength was similar for all three cases. This suggests the wake size was similar and the more negative dC_L values for the skew cases were possibly due to the asymmetry of the wake more towards the pressure peaks than for the straight through case. This was shown in the surface flow visualisation.

5 Predicting Three Dimensional Coefficient Increments from Two Dimensional Data

It is known from previous studies [1, 2] that the pressure difference between upper and lower surfaces is a key driver of damage jet characteristics, and therefore effects of different damage configurations on coefficient increments. This pressure difference will vary with obliquity and chordwise location (and with skew, if on a three dimensional wing).

The three dimensional predictive technique aims to predict the effects of damage on a wing of finite aspect ratio using two dimensional coefficient increment data and the relations to pressure difference. It is likely that the wings will not be of the same chord or area, and as such these factors must be taken into account. Work by Render et al [3] used pressure coefficient differences to relate two dimensional and three dimensional coefficient increments. Two dimensional coefficient increments were converted to three dimensional values by multiplying the two dimensional coefficients by the ratio of the two dimensional wing area to the three dimensional wing area. However, since the wings were of identical chord, the areas removed from the wing by the hole were identical. The method was extended by plotting coefficient increment areas (multiplying the increments by the wing area) against the pressure coefficient difference between the upper and lower surfaces, taken at the chordwise centre of the hole. This was found to collapse the two and three dimensional data well, but no further work was undertaken
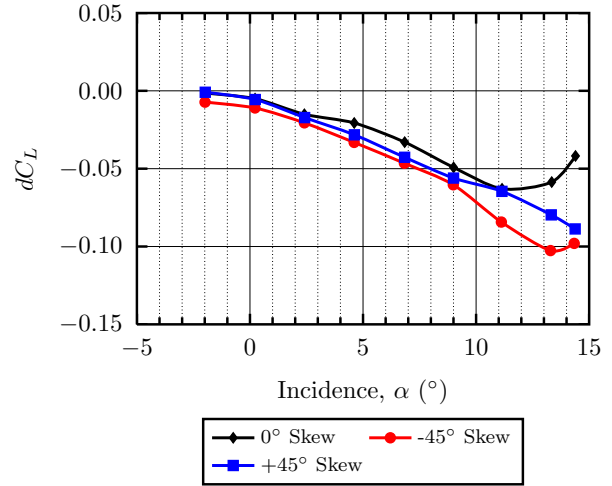

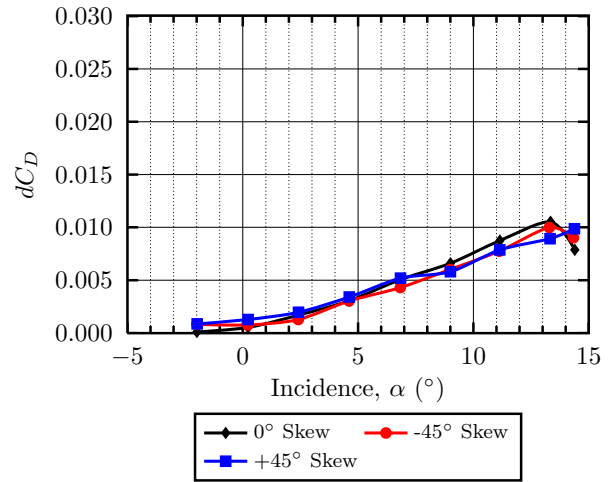**Fig. 13** Variation of dC_L with skew for a 20%c hole at the centre location

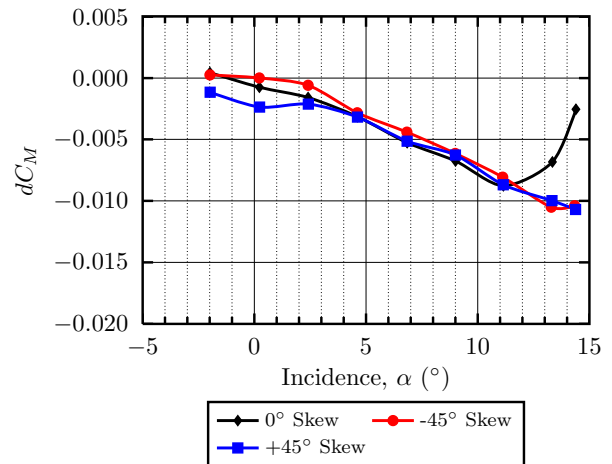**Fig. 14** Variation of dC_D with skew for a 20%c hole at the centre location

Fig. 15 Variation of dC_M with skew for a 20%c hole at the centre location

to predict the coefficient increments. It was necessary to significantly modify this original method in order to account for different chord sizes, particularly with regards to converting two dimensional data to three dimensional values.

5.1 Refinement of Pressure Difference Selection

The pressure difference required for use in the predictive technique is defined as the difference in surface pressure coefficients between the upper and lower surfaces. The pressures are taken from the chordwise locations of the damage hole, and will therefore be at different locations for oblique cases. All previous predictive techniques [2, 3] had used a very basic method of obtaining the pressure coefficient difference. This involved simply using the pressure at the chordwise centre of the damage hole. For smaller holes this may prove sufficiently accurate, but would not have acceptable accuracy with larger holes, or holes closer to the pressure peak, due to the larger changes in pressure across the hole.

In order to provide a more accurate pressure coefficient difference, the pressures were area-weighted across the hole. This method was sufficiently adaptable to be applied to a two or three dimensional wing, with varying chordwise and spanwise pressure. The hole was divided into a number of small squares, n. Each square had an area and pressure coefficient associated with it, and where necessary the pressure coefficient was interpolated. Equation 4 was used to calculate the pressure coefficient across the hole, $C_{p\ hole}$, by integrating pressures across the area of the hole.

$$C_{p\ hole} = \frac{\sum \left(\Delta C_{p\ n} \cdot \Delta A_n \right)}{\sum \Delta A_n} \qquad (4)$$

It was found that using a square size of approximately 0.25%c provided an area within 3% accuracy of the hole area, and a $C_{p\ hole}$ value that had converged to within four decimal places, without leading to excessive processing times.

5.2 Variation of Coefficient Increments with Pressure

Figures 16 to 18 show the variation in lift, drag and pitching moment coefficient increments, respectively, with the pressure coefficient difference between upper and lower holes for all two dimensional damage cases using 20%c holes. As can be seen from the three figures there is a distinct trend with coefficient increments increasing in magnitude as the pressure coefficient difference becomes more negative. The degree of scatter on the coefficient increment plots gives confidence to using relationships between dC_p and coefficient increments.

The correlation between the coefficient increments and dC_p supports the use of pressure coefficient differences to normalise data sets. It is interesting to note that when collapsing the data in this way there is no real distinction between weak and strong jets. This simplifies any predictive technique as it does not require prior knowledge of the transition points from weak to strong jet. As a result, a single prediction can be used, rather than predicting weak jet and strong jet conditions separately.

5.3 Conversion of Two Dimensional Coefficient Increments to Three Dimensional Values

When the damage hole area is expressed as a function of the chord, the converted three dimensional lift, drag and pitching moment coefficient increments (indicated with a subscript '3Dc') can be obtained from two dimensional coefficient increments using the three formulae shown in Equations 5 to 7. These formulae are valid for models of different spans and chords, provided the damage holes on both wings are of the same diameter, when expressed as a percentage of the chord. The formulae do not yield final three dimensional coefficient increments.

$$dC_{L3Dc} = dC_{l2D} \left(\frac{b_{2D}}{c_{2D}} \right) \left(\frac{c_{3D}}{b_{3D}} \right) \qquad (5)$$

$$dC_{D3Dc} = dC_{d2D} \left(\frac{b_{2D}}{c_{2D}} \right) \left(\frac{c_{3D}}{b_{3D}} \right) \qquad (6)$$
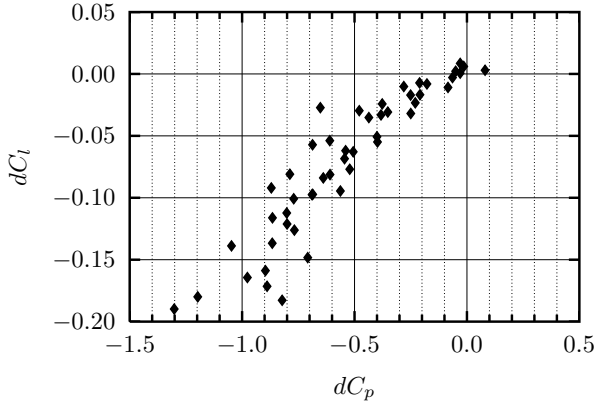
Fig. 16 Variation of two dimensional lift coefficient increment with pressure coefficient difference, for a 20%c diameter hole with a range of obliquity angles
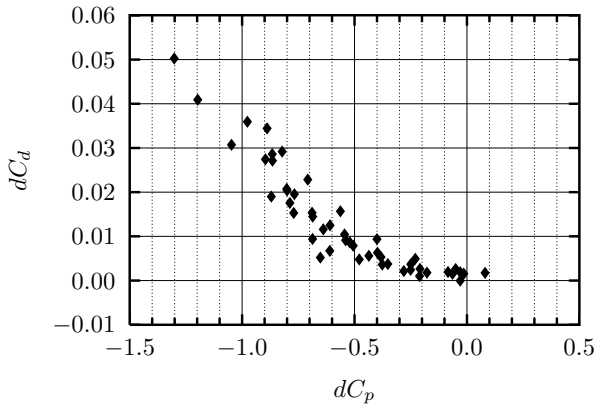

Fig. 17 Variation of two dimensional drag coefficient increment with pressure coefficient difference, for a 20%c diameter hole with a range of obliquity angles
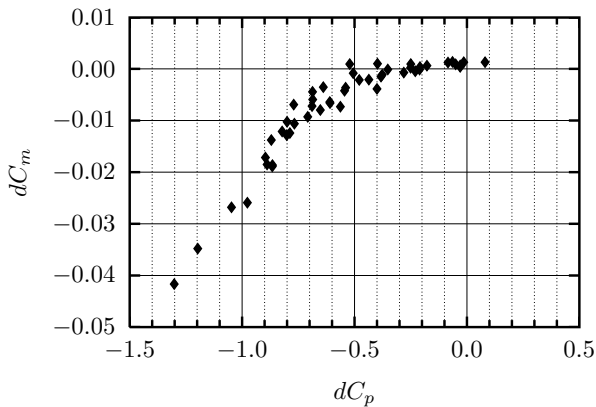

Fig. 18 Variation of two dimensional pitching moment coefficient increment with pressure coefficient difference, for a 20%c diameter hole with a range of obliquity angles

$$dC_{M_{3Dc}} = dC_{m_{2D}} \left(\frac{b_{2D}}{c_{2D}} \right) \left(\frac{c_{3D}}{b_{3D}} \right) \qquad (7)$$

To make use of the outputs from Equations 5 to 7 in the prediction methodology, it is necessary to obtain pressure coefficient differences, dC_p, from undamaged pressure distributions, using the method outlined in section 5.1. These values are required for the two dimensional and three dimensional wings at the chordwise locations of the damage hole. The three dimensional experimental increments can be collapsed for span by plotting against the undamaged pressure coefficient differences, dC_P. When the converted two dimensional increments (Equations 5 to 7) were plotted against the two dimensional undamaged pressure coefficient differences, dC_p, it was found that the converted two dimensional data matched well with the collapsed three dimensional data. This is shown in Figures 19 to 21 for converted lift, pitch and drag coefficient increments respectively. From these figures, the converted coefficient increments can be interpolated to obtain the predicted three dimensional coefficient increments. Figure 22 shows the variation of three dimensional dC_P values with incidence and spanwise location for two oblique cases. This figure is used to obtain discrete three dimensional dC_P values for each incidence. These dC_P values are then used to interpolate dC_L, dC_D and dC_M from the converted two dimensional data in Figures 19 to 21. The converted two dimensional data set is extrapolated where necessary.

Figures 19 to 21 show how the lift, drag and pitching moment coefficient increments for the two dimensional case collapse onto the three dimensional data at the three spanwise locations when plotted against the pressure coefficient difference. As can be seen, the lift and drag coefficient increments collapse very well, giving confidence to the prediction method. The pitching moment coefficient increment, however, has a significant offset. Small errors in the pitching moment may have been introduced due to different model mounting configurations. Comparing the results to those of Render et al [3] show that a similar trend is identified

with the pitching moment coefficient increment plots. Render et al identified a significant offset between pitching moment data from a wing of aspect ratio 6 and converted two dimensional data which was not presence at higher aspect ratios. This used a different aerofoil, chord, span and hole size, but was tested in the same wind tunnel. The trend appears similar with that shown in Figure 21, and suggests a possible issue with the half model configuration when used with lower aspect ratio wings.

5.4 Review of Accuracy

To validate the accuracy of the prediction technique, wind tunnel data for straight through, $\pm 60°$ obliquity and $+45°$ skew at the central location of the three dimensional wing is compared against predictions from the two dimensional data. Reference should be made to the repeatability bands given in Table 1. Converting the two dimensional repeatability coefficients to converted three dimensional coefficients using Equations 5 to 7 gives:

- $C_{L_{3Dc}} = \pm 0.014$

- $C_{D_{3Dc}} = \pm 0.0012$

- $C_{M_{3Dc}} = \pm 0.0016$

Figures 23 to 26 show the experimental and predicted lift coefficient increments with $0°$, $+60°$ and $-60°$ obliquity and $+45°$ skew respectively. The figures show a generally good match between the predictions and the experimental results. For $+60°$ obliquity (Figure 24) it can be seen that the prediction begins to break down beyond approximately $+8°$. This is due to the jet not continuing to strengthen as incidence increased, as previously discussed. Divergence is noticed for higher incidences with the $-60°$ obliquity case (Figure 25), limiting the accuracy of the method to lower incidences.

Figures 27 to 30 show the experimental and predicted three dimensional drag coefficient increments for the four cases being considered. The predicted drag coefficient increments do not show as good a match to the experimental data as
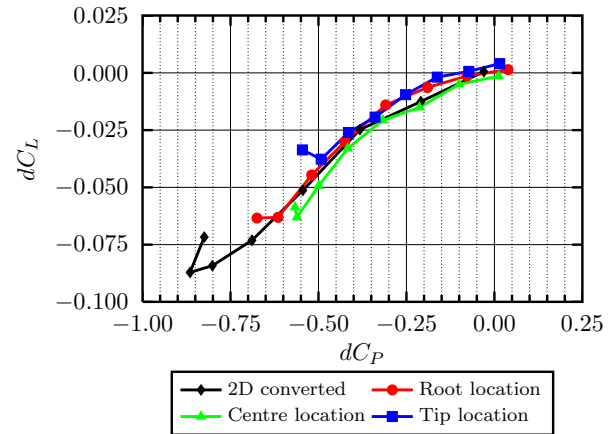
Fig. 19 Comparing predicted two dimensional $dC_{L_{3Dc}}$ values with actual three dimensional values at three spanwise locations for a 20%c straight through hole
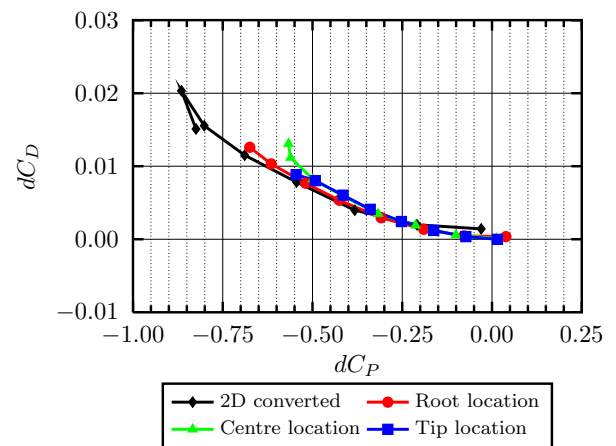

Fig. 20 Comparing predicted two dimensional $dC_{D_{3Dc}}$ values with actual three dimensional values at three spanwise locations for a 20%c straight through hole
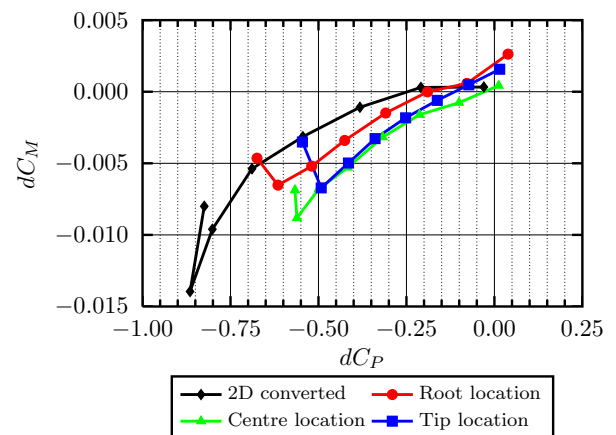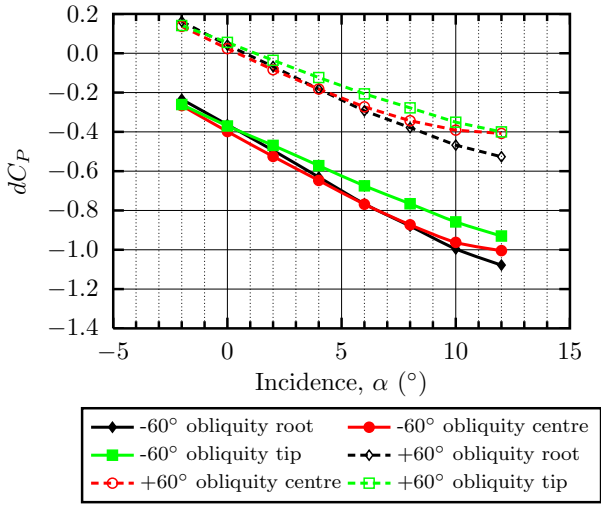

Fig. 21 Comparing predicted two dimensional $dC_{M_{3Dc}}$ values with actual three dimensional values at three spanwise locations for a 20%c straight through hole

Fig. 22 Variation of undamaged dC_P across a 20%c hole with incidence and spanwise location for different oblique cases on a three dimensional wing
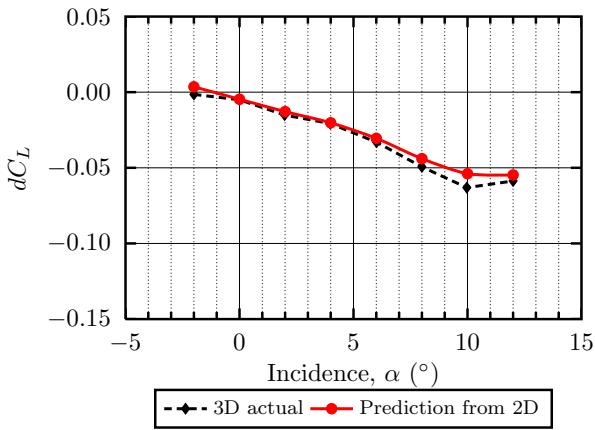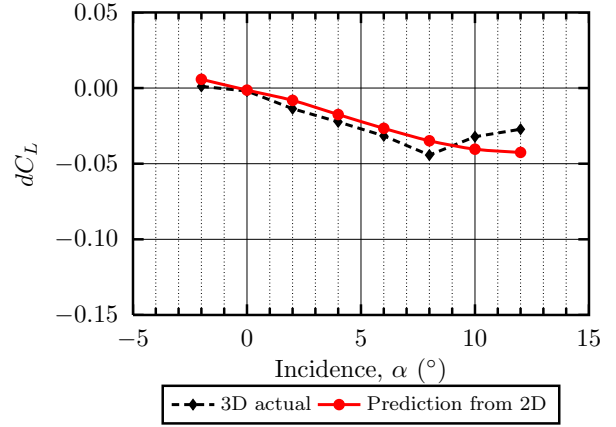

Fig. 24 Prediction of dC_L for a 20%c hole with +60° obliquity from two dimensional data, with comparison against three dimensional experimental data
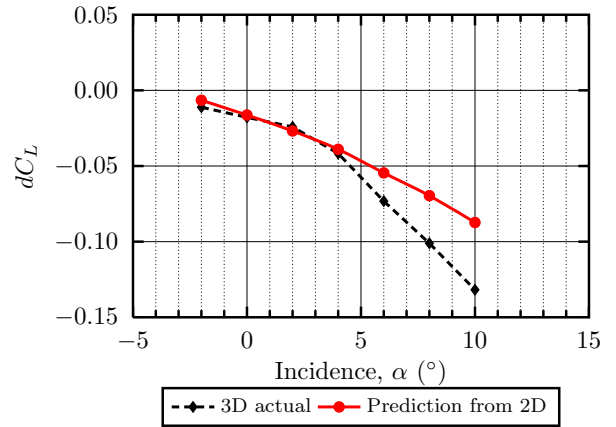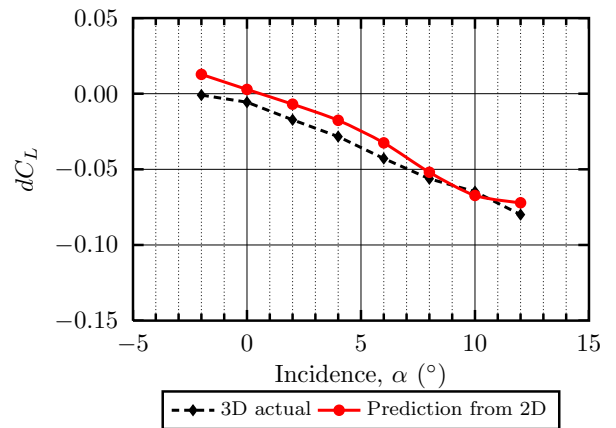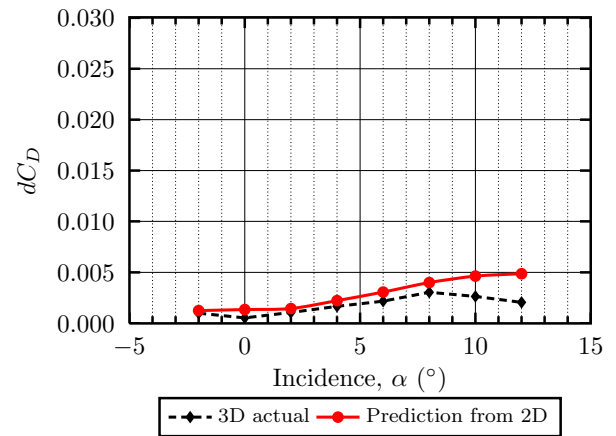

Fig. 25 Prediction of dC_L for a 20%c hole with -60° obliquity from two dimensional data, with comparison against three dimensional experimental data

Fig. 23 Prediction of dC_L for a 20%c straight through hole from two dimensional data, compared with three dimensional experimental data

Fig. 26 Prediction of dC_L for a 20%c hole with +45° skew from two dimensional data, with comparison against three dimensional experimental data

Fig. 27 Prediction of dC_D for a 20%c straight through hole from two dimensional data, compared with three dimensional experimental data

Fig. 28 Prediction of dC_D for a 20%c hole with +60° obliquity from two dimensional data, with comparison against three dimensional experimental data

the lift coefficient increments. There is a general trend in that the prediction under-estimates more significantly as obliquity becomes more negative. This is likely due to differing wake structures, since the under predictions are most significant at the higher incidences, when strong jets are present. The differences in wakes are likely as a result of the asymmetry introduced by the presence of the wing tip.

Figures 31 to 34 show the experimental and predicted three dimensional pitching moment coefficient increments for the four cases. The pitching moment coefficient increments show the greatest error between the prediction and actual results. As mentioned earlier this is consistent with findings by Render et al [3]. Data from Render et al suggests that this is a result of testing lower aspect ratio wings in half model configuration, as the offset was not present for aspect ratios of 8 or 10. Therefore, any predictions made for wings with an aspect ratio below 8 will be subject to large errors in the pitching moment coefficient increments.

The preceding figures indicate that generally, the conversion and prediction method is suitable, although difficulty exists in applying it to lower aspect ratio wings when considering pitching moment coefficient increments. Errors were apparently reduced with the +60° obliquity case, primarily due to the smaller coefficient
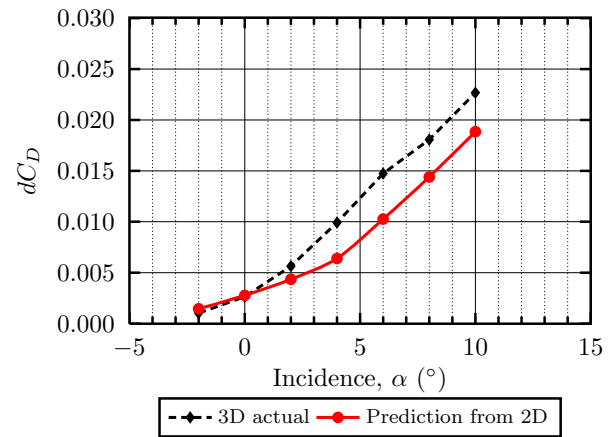

Fig. 29 Prediction of dC_D for a 20%c hole with -60° obliquity from two dimensional data, with comparison against three dimensional experimental data
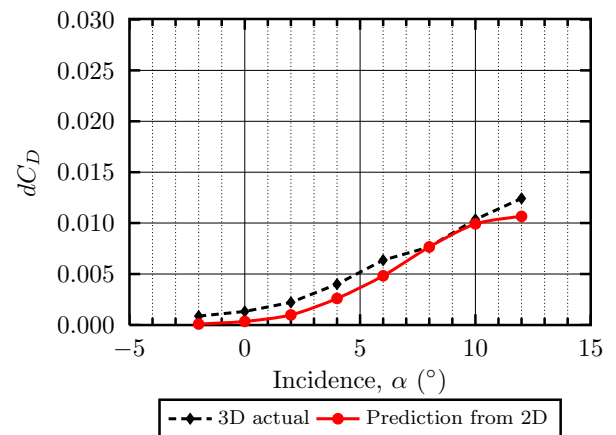

Fig. 30 Prediction of dC_D for a 20%c hole with +45° skew from two dimensional data, with comparison against three dimensional experimental data
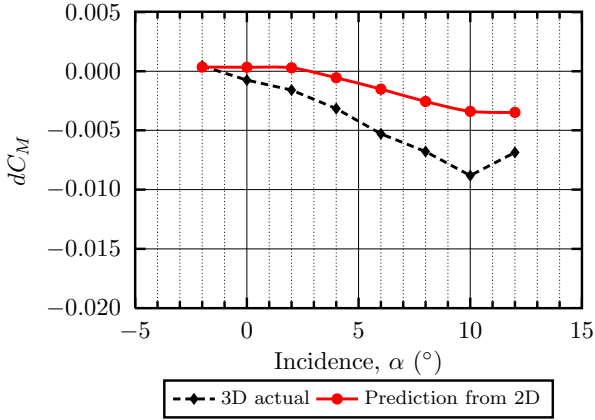
Fig. 31 Prediction of dC_M for a 20%c straight through hole from two dimensional data, compared with three dimensional experimental data
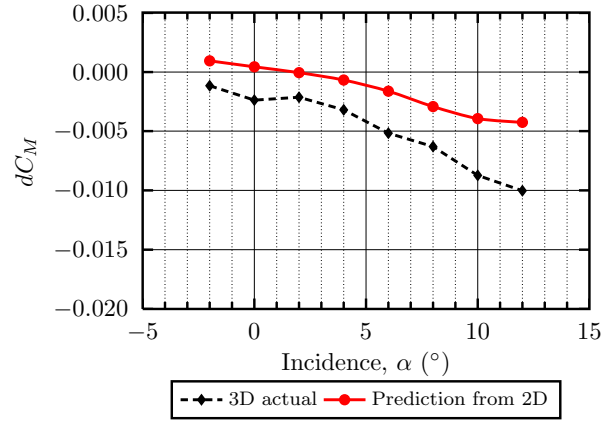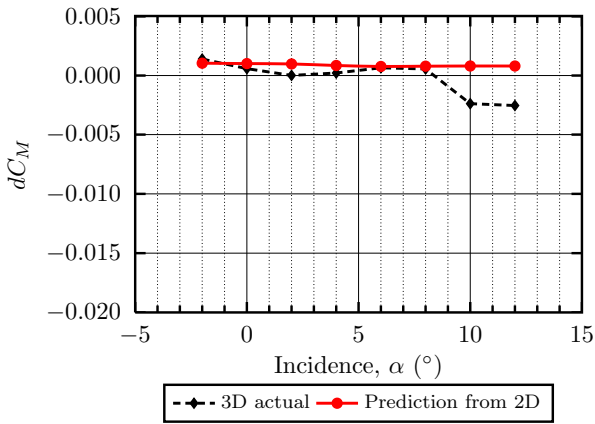

Fig. 32 Prediction of dC_M for a 20%c hole with +60° obliquity from two dimensional data, with comparison against three dimensional experimental data
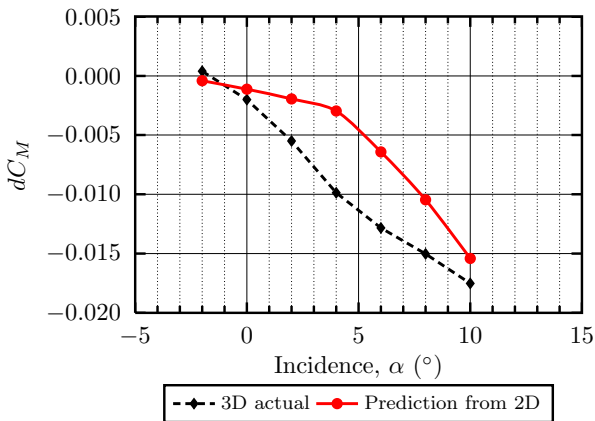

Fig. 33 Prediction of dC_M for a 20%c hole with -60° obliquity from two dimensional data, with comparison against three dimensional experimental data

Fig. 34 Prediction of dC_M for a 20%c hole with +45° skew from two dimensional data, with compari-son against three dimensional experimental data

increments. The predictions for lift were very encouraging, with limits only required on the +60° obliquity case, due to the different performance of the jet. Limitations were encountered with the drag coefficient increment when the jet was at its strongest, and the prediction generally performed better with weaker jets. Future work may include the investigation of an additional parameter to take into consideration the size of the wake.

6 Conclusions

1. General trends from previous publications were confirmed. The effects of battle damage were seen to increase with incidence and chordwise hole orientation. The effects witnessed on a three dimensional wing were consistent with those from two dimensional testing.

2. When battle damage was applied to a wing of finite aspect ratio, the effects were weakened towards the tip, and asymmetry was introduced into the flow as a result of the spanwise variation in pressure differential.

3. The effects due to damage witnessed on a three dimensional wing were consistent with those from two dimensional testing and were not dependent on Reynolds Number.

14

4. The pressure coefficient difference between upper and lower surface holes could be used to aid predicting three dimensional values from two dimensional data with reasonable accuracy.

5. Prediction techniques were found to be independent of whether the jet was weak or strong, allowing the same method to be used for both cases.

6. The prediction technique provided a good degree of accuracy when predicting lift coefficient increments. Drag coefficient increments were generally under predicted. The pitching moment coefficient increment predictions were of relatively poor accuracy but this was found to be likely due to effects from a small aspect ratio wing.

Acknowledgements

References

[1] Render, P. M. and Pickhaver, T. W. *The influence of hole orientation on the aerodynamics of battle damaged wings*. AIAA 30th Applied Aerodynamics Conference, AIAA-2012-2890, June 25–28 2012,

[2] Irwin, A. J. *The influence of mid-chord battle damage on the aerodynamic characteristics of two-dimensional wings*. The Aeronautical Journal, Volume 104, No. 1033, pp 153–161, 2000

[3] Render, P. M; Samad-Suhaeb, M; Yang, Z and Mani. *Aerodynamics of battle-damaged finite-aspect-ratio wings*. Journal of Aircraft, Volume 46, May–June 2009

[4] Robinson, K. W. and Leishman, J. G. *Effects of ballistic damage on the aerodynamics of helicopter rotor airfoils.* Journal of Aircraft, Volume 35, September–October 1998

[5] Irwin, A. J. and Render, P. M., *The influence of internal structure on the aerodynamic characteristics of battle-damaged wings.* AIAA 14th Applied Aerodynamic Conference, AIAA-1996-2395 June 17–20 1996

Copyright Statement